ELSEVIER

Organic Electronics 2 (2001) 97–104

Organic Electronics

www.elsevier.com/locate/orgel

# Interface electronic structure of organic semiconductors with controlled doping levels

J. Blochwitz [a,*], T. Fritz [a], M. Pfeiffer [a], K. Leo [a], D.M. Alloway [b], P.A. Lee [b], N.R. Armstrong [b]

[a] *Institut für Angewandte Photophysik, Technische Universität Dresden, 01062 Dresden, Germany*
[b] *Department of Chemistry, University of Arizona, Tucson, AZ 85721, USA*

Received 15 January 2001; received in revised form 11 June 2001; accepted 11 June 2001

**Abstract**

We investigate the properties of inorganic–organic interfaces by ultraviolet and X-ray photoemission spectroscopy (UPS and XPS) and transport experiments. In particular, we study the interface between inorganic conductive substrates and organic layers that are intentionally p-type doped by co-evaporation of a matrix material and acceptor molecules. The photoemission spectra clearly show that the Fermi levels shift due to the doping and that the space charge layer width changes with doping (high doping – small width). The changes in the electronic structure of the interface due to doping agree well with results of transport experiments. © 2001 Elsevier Science B.V. All rights reserved.

*PACS:* 73.40.Ns; 73.30.+Y; 73.20.At
*Keywords:* UPS; XPS; Organic Schottky junctions; Doped layers; Organic light emitting diodes; Energy scheme

## 1. Introduction

Organic thin films with semiconducting properties have been intensively investigated in the last years (see e.g. [1,2]) due to very promising applications, such as organic light emitting diodes (OLEDs) [3,4]. In virtually any electronic device containing organic semiconductors, contacts to metals and other inorganic conductors play a crucial role. Despite the advances in device application, there is still only limited understanding of the interface between organic materials and contacts. A number of recent studies have helped to understand basic properties of the interfaces (see e.g. the review by Seki et al. [5]). In particular ultraviolet and X-ray photo emission spectroscopy (UPS and XPS) have been used to investigate metal/organic [6–9] and organic/organic [10–14] interfaces. The organic layers employed in such studies were *nominally undoped*, although the purity of organic layers is usually insufficient to achieve intrinsic behavior. For the breakthrough of inorganic semiconductor devices, controlled doping was a key step: Fermi level control is crucial for pn-junctions, high built-in voltages (which is important, e.g., for efficient solar cells), and for well-defined ohmic or blocking contacts with

* Corresponding author.
*E-mail address:* blochw@iapp.de (J. Blochwitz).


PII: S1566-1199(01)00016-7

metals or other conductive substrates. Metal–inorganic semiconductor contacts (Schottky contacts) have been extensively investigated and are rather well understood (see e.g. [15,16]).

Doping of organic semiconductors has only been scarcely addressed so far [17–21]. We have recently investigated the controlled doping of organic layers by conductivity and thermo-power studies and have shown that significant Fermi level shifts and comparatively high conductivities can be achieved by co-evaporation of matrix and acceptor (or donor) molecules [22,23]. Doping leads to significantly improved properties of devices with organic layers, e.g., better carrier injection, more efficient carrier transport and hence lower operating voltage in OLEDs [24,25]. Phenomenologically dopability of such layers is rather similar to inorganic semiconductors but the microscopic mechanisms seem to be different [26].

Here we present the first study of the electronic structure of interfaces between inorganic contact materials and molecular organic semiconductors with controlled doping. In particular, we investigate contacts between indium–tin oxide (ITO) or gold (Au) and p-doped zinc–phthalocyanine by UPS and XPS as well as by current–voltage transport measurements on diode structures. We clearly observe highest occupied molecular orbital (HOMO), XPS-peak and vacuum level shifts due to space charge layers (or level bending), with a width decreasing by doping. Additionally, interface dipoles are observed with a potential drop largely independent of doping. The distance between the Fermi level and the HOMO [1] decreases with doping. For the doped material the level bending behavior can be well explained by space charge formation, analogous to the effect occurring upon doping of inorganic semiconductors. The electrical transport properties of the junctions agree well with the observed electronic structure.

## 2. Experiment and data analysis

The organic layers were vapor deposited with growth rates of 2–6 Å/min for the matrix molecules and 0.1–0.2 Å/min for the dopants. The investigated thickness range was 2 Å for the first layer up to approximately 200 Å for the thickest layers. Doped layers were prepared by co-evaporation of matrix (zinc–phthalocyanine – ZnPc (Aldrich), purified by zone sublimation) and dopant (tetrafluoro-tetracyano-quinodimethane – $F_4$-TCNQ (Aldrich), used as provided, for the molecular formula see inset of Fig. 1). The molar doping ratio for the doped samples is approximately 1:30. The substrates (ITO on glass, and poly-crystalline Au-foil) were ultrasonically cleaned in chloroform, acetone and alcohol, left in vacuum for one night and were Ar-sputtered shortly before evaporation of the first organic layer. The organic layer was made in several growth steps in order to sequentially vary the layer thickness, with transfer to the analyzer chamber (base pressure $10^{-9}$ mbar) and UPS and XPS characterization between each growth step. UPS experiments were done with a 21.21 eV He(I) source at 5 eV pass energy and with −5 V bias voltage applied to the sample to separate

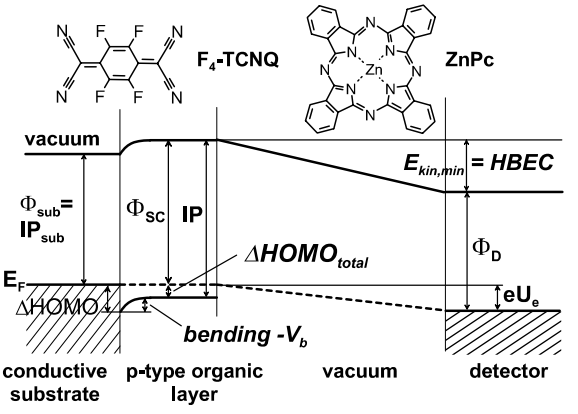


Fig. 1. Energy level scheme of a metal–organic interface in an UPS/XPS experiment. See text for a detailed description. The inset shows the chemical structure of the organic materials used in this study.

[1] We would like to stress here that due to both, solid state effects and intramolecular electronic relaxation, one can of course not measure the HOMO position (as characteristic of a single molecule) in organic thin films but the energetic position of the valence electrons. However, this energy level is somehow related to and derived from the HOMO level of an isolated molecule, and will therefore be called 'HOMO peak' for short in this paper.

secondary electrons originating from sample and spectrometer [27]. XPS measurements were carried out with a 1486.6 eV monochromatic Al-K$\alpha$ radiation at a typical pass energy of 10 eV. The evaluation of the data followed the scheme described by Schlaf et al. [11]. The XPS peak positions and widths were determined by fitting the data with Gaussian/Lorentzian (70:30) line shapes. For the UPS data, the low kinetic energy cut-off (= high binding energy cut-off, HBEC) was determined by the energy-axis intersection of a straight line fitted to the slope of the spectra (between $\approx$30% and 70% of its height). The Fermi energy positions $E_F$ of the conductive substrates were obtained as the center of the Fermi edge slopes.

To deduce the ionization potential from the width of the photoionization spectra we measured the high kinetic energy cut-off of the HOMO peak instead of the HOMO peak maximum. This is for the following reasons: (i) The HOMO cut-off is a physically reasonable value since the analyzer broadening can be neglected (from the width of the Au-Fermi edge the analyzer resolution was estimated to be $<$50 meV) compared to the peak broadening due to inherent layer properties such as electronic band width and vibronic excitations. (ii) We believe that for the explanation of transport and injection phenomena in organic Schottky junctions the adiabatic energy transition (the final state of the molecular crystal after photoionization process is the phononic ground state) is the relevant one. This HOMO cut-off ($E_{\mathrm{HOMO}}^{\mathrm{cut\text{-}off}}$) was determined by fitting a straight line to the slope of the (background corrected) HOMO peak.

We discuss our results in the framework of the scheme shown in Fig. 1. Values which can be directly taken from the UPS-spectra are $E_{\mathrm{kin}}^{\mathrm{min}}$ (or HBEC), the difference $\Delta$HOMO of the HOMO cut-off energy to the Fermi energy of the underlying substrate and the ionization potential IP. The latter is calculated from the energetic width of the whole spectrum of the photoemitted electrons,

$$\mathrm{IP} = 21.21\ \mathrm{eV} - (E_{\mathrm{kin}}^{\mathrm{max}} - E_{\mathrm{kin}}^{\mathrm{min}}). \tag{1}$$

For the conductive substrate, $E_{\mathrm{kin}}^{\mathrm{max}}$ is the kinetic energy of the photoelectrons emitted from the Fermi edge of the conductive substrate ($E_{\mathrm{F,sub}}$), for the organic over-layer $E_{\mathrm{HOMO}}^{\mathrm{cut\text{-}off}}$ is taken as $E_{\mathrm{kin}}^{\mathrm{max}}$. With the assumption of Fermi level alignment over the entire organic layer [2] the total energy balance equation of the measuring system is

$$E_{\mathrm{kin}}^{\mathrm{min}} = \Phi - \Phi_{\mathrm{D}} - eU_{\mathrm{e}}, \tag{2}$$

where $U_e$ is the external voltage (in our case $-5$ V), $\Phi_D$ the detector work function and $\Phi$ the work-function of the outermost layer. Without an organic coverage, $\Phi$ is the work-function of the substrate $\Phi_{\mathrm{sub}}$ which equals the ionization potential $\mathrm{IP}_{\mathrm{sub}}$ and hence the actual detector work function can be calculated,

$$\Phi_{\mathrm{D}} = \mathrm{IP}_{\mathrm{sub}} - E_{\mathrm{kin,sub}}^{\mathrm{min}} - eU_{\mathrm{e}}. \tag{3}$$

Then the work-function $\Phi = \Phi_{\mathrm{SC}}$ at a certain thickness of the organic semiconductor over-layer can be obtained from the HBEC. Eqs. (1)–(3) yield

$$\begin{aligned}\Phi_{\mathrm{SC}} &= E_{\mathrm{kin}}^{\mathrm{min}} + \mathrm{IP}_{\mathrm{sub}} - E_{\mathrm{kin,sub}}^{\mathrm{min}} \\ &= E_{\mathrm{kin}}^{\mathrm{min}} + 21.2\ \mathrm{eV} - E_{\mathrm{F,sub}}.\end{aligned} \tag{4}$$

To obtain the energy alignment of the metal/organic hetero-junctions, we measure the development of the HBEC and the HOMO peak cut-off in the UPS spectra and of the shifts of suitable element peaks in the XPS spectra as the thickness of the topmost organic layer is increased. From these values, we deduce the difference $\Delta\mathrm{HOMO}_{\mathrm{total}}$ between the substrate Fermi energy and the HOMO cut-off energy of the thickest organic over-layer (assuming that at this stage no further shifts of the spectra take place), the ionization energy $\mathrm{IP}_{\mathrm{organic}}$ for a thick over-layer, the difference of the HBEC between thick organic layer and substrate ($\Delta E_{\mathrm{HBEC}}$) and the total level bending $V_{\mathrm{b,total}}$ during the development of the space charge region in the organic layer near the substrate. The term "level bending", as we use it here, is an equivalent of the expression "band bending" used for inorganic semiconductors. One needs to keep in mind that the underlying physical process might not be similar to band bending, in particular in case of nominally undoped organic layers on metals

[2] The conductivity of both, the undoped and the doped layers, is by far large enough to ensure dielectric relaxation, i.e. Fermi level alignment, before data are taken.

[28]. As we will see later, the terms level or band bending very well describe our experimental findings for the Schottky junction between doped organic layers and conductive substrates. To determine the level bending, we consider only the XPS peak shifts, since (i) for the UPS high binding energy cut-off the influence of level bending and dipole layer effects is hard to distinguish, and (ii) for low organic layer thicknesses the HOMO features are superimposed with the photoemission signal from the substrate [28]. And (iii), the measurement of both XPS and UPS shifts leads to a broader database allowing a better distinction between dipole and other effects occurring directly at the interface and level bending effects in the bulk. The difference ΔHOMO between the HOMO energy of the organic material and the Fermi energy of the substrate directly at the interface can then be calculated,

$$\Delta\mathrm{HOMO} = \Delta\mathrm{HOMO}_{\mathrm{total}} - V_{\mathrm{b,total}}. \quad (5)$$

Additionally, the interface dipole energy can be obtained from

$$eD = -[\Delta E_{\mathrm{HBEC}} - V_{\mathrm{b,total}}] = -[\Delta\mathrm{HOMO} - (\mathrm{IP}_{\mathrm{organic}} - \mathrm{IP}_{\mathrm{sub}})]. \quad (6)$$

In the above equation, a negative sign for $eD$ was chosen for the case that electrons are accelerated across the interface (following [5,29]).

In summary, to conclude an energy level alignment scheme as displayed in Figs. 4 and 6 the following values had to be measured or calculated: (i) the ionization potential of the substrate (from the width of the substrate UP-spectra: Eq. (1) $\mathrm{IP}_{\mathrm{sub}}$, (ii) the ionization potential of the thick organic over-layer $\mathrm{IP}_{\mathrm{organic}}$, (iii) the distance of the HOMO cut-off energy at thick organic layer coverage to the Fermi-energy of the substrate $\Delta\mathrm{HOMO}_{\mathrm{total}}$ and (iv) the level bending value $V_{\mathrm{b}}$. The values of ΔHOMO and $eD$ can then be calculated according to Eqs. (5) and (6).

## 3. Results and discussion

Fig. 2 (left) shows the development of the UPS spectra for undoped ZnPc on ITO as a function of the ZnPc layer thickness (data are shown in an uncorrected kinetic energy scale). The lowest spectrum is for bare ITO with a Fermi edge at $E_{\mathrm{kin}} = 26.5$ eV (the signal step at the Fermi edge for ITO is smaller than for a typical Au Fermi edge, but can still be clearly resolved). The ZnPc HOMO peak appears at $E_{\mathrm{kin}} \cong 25$ eV (maximum value) and shifts slightly towards lower binding energies at higher coverage. The width of the HOMO peak does not change systematically. No other features in the energy gap range of the UPS-

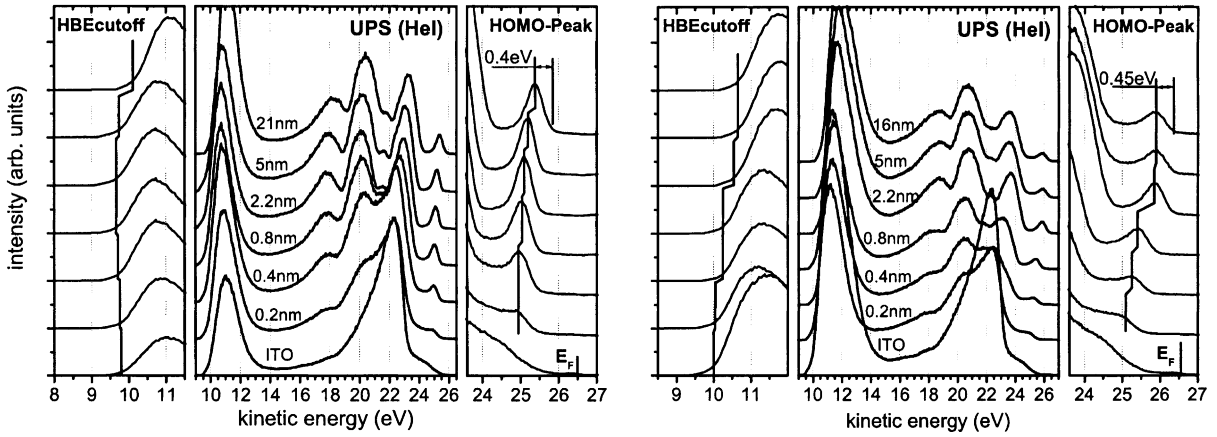


Fig. 2. UP-spectra development with increasing organic layer thickness for ZnPc on ITO (left) and $F_4$-TCNQ-doped ZnPc on ITO (right). The vertical lines mark the shifts of the high binding energy cut-off and the HOMO peak shift. The values 0.4 and 0.45 eV mark the (constant) HOMO peak width (i.e. the distance of the peak maximum to the cut-off).

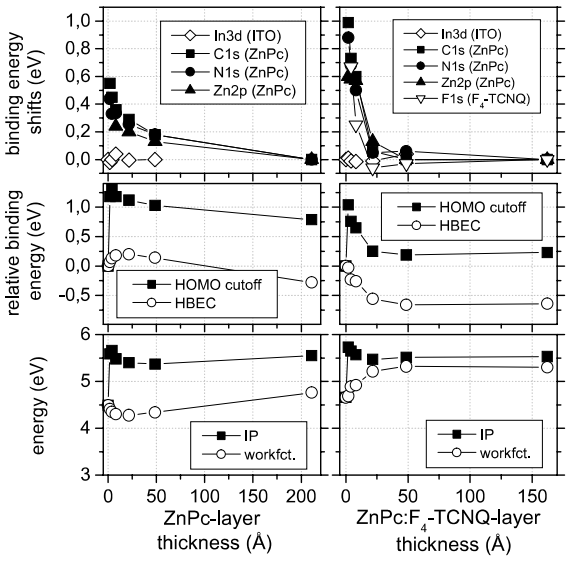


Fig. 3. UPS energy shifts and XPS peak shifts for ZnPc on ITO (left) doped ZnPc on ITO (right).

spectra are observed, which would point towards a chemical reaction at the interface or polaronic states [30]. On the high binding energy side, the cutoff first shifts slightly to higher and later back to lower binding energies, indicating an interface dipole layer (opposite to the space charge layer developing later).

Fig. 2 (right) shows the development of the UPS spectra for ZnPc doped with $F_4$-TCNQ on ITO. Again, the HOMO is shifting towards lower binding energies, together with the HBEC. UPS and XPS shifts are summarized in Fig. 3. The left column shows the undoped case of ZnPc on ITO, the right part the shifts of doped ZnPc on ITO. The top part shows all relevant XPS peak shifts in a binding energy scale. Zero shift is defined at the peak position at no coverage for the XPS peaks belonging to the substrates, and that at highest coverage for all elemental peaks belonging to the organic over-layer. The graphs in the center show the shift of the HOMO cut-off in a binding energy scale relative to the Fermi edge position of the substrate, and the change in the HBEC relative to the position of the HBEC of the substrate. The bottom graphs summarize the development of the ionization energy IP and the work-function $\Phi_{SC}$ of the organic layer. Note, that the region where UPS and XPS peak positions are changing is much smaller in the doped case, indicating a smaller space charge layer width at the interface.

Fig. 4 shows the energy diagrams derived from the photoemission data for the case of nominally undoped ZnPc (left) and for ZnPc doped with $F_4$-TCNQ (right) on ITO substrates. For determining the level bending from UPS and XPS experiments, the measurement of the peak position at very low coverage is an intrinsic problem. We thus took for the level bending values a mean value of the peak positions which were reliably observable for the lowest coverage (namely the C1s and N1s peaks). For the experiments discussed here, the HOMO peak shift agrees with the level bending values obtained from XPS within the error span. In both the undoped and the doped case, we observe an interface dipole leading to a potential difference of about −0.3 eV, with a direction corresponding to electron transfer to the ITO. It should be noted

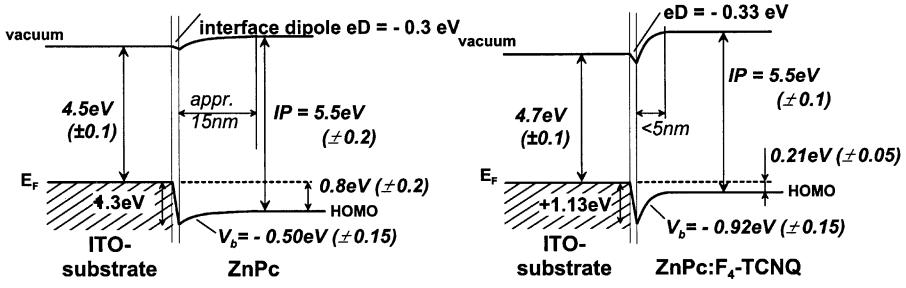


Fig. 4. Energy level scheme as obtained from UPS and XPS for the contact between ITO and ZnPc. The left side shows the energetic structure for the undoped case; the right side for ZnPc p-doped with $F_4$-TCNQ.

here that for nominally undoped ZnPc on ITO the change of the peak positions between 50 and 200 Å must be caused by extrinsic effects like a degradation of the less conductive organic layer. It cannot be a simple sample charging effect since the peaks shift towards lower binding energies. Nevertheless, taking 50 Å as maximum organic layer thickness before these effects start to play a role would lead to a lower ionization potential of the ZnPc-layer, but at the same time to a lower level bending $V_b$ and a higher distance of the HOMO level to the Fermi-level $\Delta HOMO_{total}$ as compared to the data given in Fig. 4 (left part). This would result in similar values for the HOMO difference $\Delta HOMO$ directly at the interface and the dipole energy $eD$ at the interface. The possible extrinsic effects is accounted for by the larger experimental errors given in Fig. 4 for the ionization potential $IP_{organic}$ and the total HOMO shift $\Delta HOMO_{total}$ as compared to doped ZnPc on ITO, where charging and degradation can be ruled out by the very high conductivity of these doped films.

The main observations are: (i) The Fermi level in the doped ZnPc layer is shifted toward the HOMO states by about 0.6 eV, compared to the undoped case, clearly showing the effect expected for p-type doping [22]. (ii) Accordingly, we see a much higher level bending in the doped sample compared to the undoped one. (iii) The width of the space charge layer is strongly reduced in the doped sample, compared to the undoped one. Although these values are more qualitative, one clearly sees a reduction of the width of the space charge layer from >15 nm in the undoped to <5 nm in the doped case. With the observed level bending of $V_b = -0.9$ eV and the nominal doping ratio of 1:30 ($N_A = 1/30\ N_{mol} \approx 5 \times 10^{25}\ m^{-3}$, assuming that all dopants are active and all matrix molecules (density $N_{mol}$) provide one charge transport level), the width $w$ of the space charge layer can be calculated from standard semiconductor theory (e.g. [31]) to

$$w = \sqrt{\frac{2\varepsilon\varepsilon_0}{e}\frac{1}{N_A}V_b}. \tag{7}$$

Choosing $\varepsilon = 4$ [32] results in a width $w$ of the space charge layer for the doped sample of 2.8 nm, which is in reasonable agreement with the experiment. Nevertheless, the origin of the level bending in the undoped case remains unclear since a much wider space charge layer than 15 nm should be observed. For intrinsic organic layers on metal substrates the origin of such a behavior is still a controverse subject in literature (e.g. compare [28,33,34] and [30,35,36]). Additionally, it should be noted here that the growth mode of the organic layers investigated is not changed below doping ratios of 5% [26]. (iv) The interface dipole is of the same sign and of very similar magnitude as compared to the case of the undoped ZnPc, which demonstrates that there is no significant accumulation of charged dopant molecules at the interface and the interface dipole is mainly caused by a charge transfer between ZnPc and ITO. (v) The ionization potential is not affected by doping [3] [37].

Fig. 5 summarizes the UPS/XPS experiments of ZnPc on a polycrystalline Au-substrate and of $F_4$-TCNQ-doped ZnPc on the same substrate. In this case the level bending (taken from the XPS peak shifts) is inversed upon doping. The F1s XPS-peak for ZnPc doped with $F_4$-TCNQ on Au was very weak compared to the F1s peak on ITO. This effect points towards a reaction of the fluor substituents at the Au-surface, which might also be reflected in the behavior of the HOMO cut-off and the HBEC at thicknesses below 20 Å.

Fig. 6 shows the corresponding energy level alignment diagrams for undoped and doped ZnPc on an Au-substrate. Again, the distance of the Fermi level to the HOMO level is decreased by doping from 1 down to 0.25 eV. Generally, because of the higher work function of Au as compared to ITO we expect an ohmic behavior for the Au–semiconductor contact. This is indeed the case for the undoped sample (left), where an accumulation layer near the interface is observed (positive level bending), together with an interface dipole 0.15 eV higher, but in the same direction, as for the

[3] The ITO ionization potential differs for the undoped and doped case, although it is physically the same substrate treated by the same cleaning procedure. It is known from literature, however, that the ITO workfunction can change dramatically by small surface modifications.

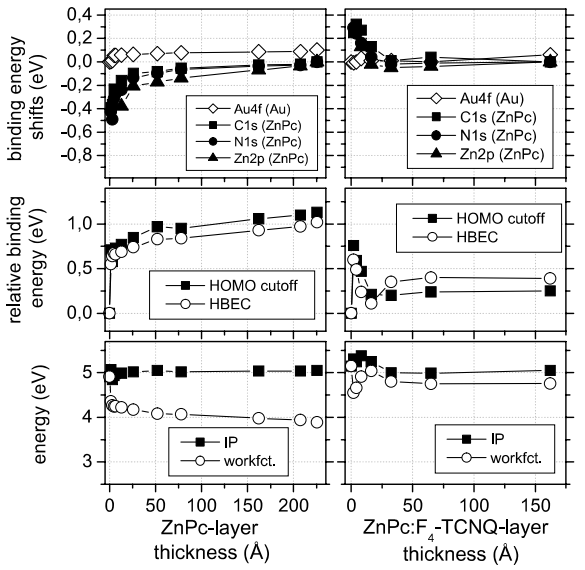


Fig. 5. UPS energy shifts and XPS peak shifts for ZnPc on Au (left) and $F_4$-TCNQ doped ZnPc on Au (right).

ITO substrate. For the doped layer (right side of Fig. 6), however, the shift of the Fermi level leads to a depletion layer near the interface, caused by a level bending in the opposite direction as compared to the undoped case. Note that the interface dipoles of the doped and undoped sample change according to the work-function change of the substrate, which implies that doping does not change the interface dipole (which is surprising taking into account the possibility of a reaction of F with Au at the interface into account). Although the ionization potential does not depend on doping, it is approximately 0.45 eV lower (5.05 eV) for ZnPc on Au than for ZnPc on ITO (5.5 eV). The reason for this behaviour is not clear (different ZnPc growth modes on the ITO and on the Au-substrate would be a possible explanation), but our conclusions regarding the doping effect remain unaffected.

For comparison, we have performed transport experiments on samples with contacts between gold and doped ZnPc which confirm the results of the UPS/XPS study and show how the contact properties can be adjusted by doping: Nominally undoped ZnPc forms an ohmic contact with Au (see [38,39]), whereas p-doped ZnPc leads to a weakly blocking contact, which is expected from the band bending caused by the downward shift of the Fermi level. The contact behavior of doped ZnPc to Au was determined from current–voltage measurements on the sample structure: Au/60 nm undoped ZnPc/440 nm doped ZnPc/Au (preparation and measurements under high vacuum). The additional 60 nm thin undoped ZnPc layer was needed to increase the width of the space charge layer so that the weak blocking behavior of the Au/doped ZnPc junction could be seen (compare [40] for the same experiments on vanadyl–phthalocyanine). Choosing the Au contact near the undoped inter-layer as anode, injection-limited rather than space charge limited currents were seen under positive bias in a voltage range between 1 and 5 V.

## 4. Summary

We have performed UPS/XPS experiments with p-doped and with undoped ZnPc layers on ITO

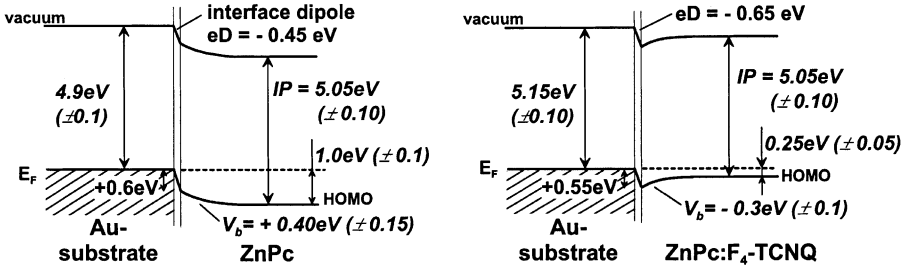


Fig. 6. Energy level scheme as obtained from UPS and XPS for the contact between Au and ZnPc. The left side shows the energetic structure for the undoped case; the right side for ZnPc p-doped with $F_4$-TCNQ.

and Au. The main observation is that by doping the Fermi level is strongly shifted to the HOMO level on both substrates. For the doped case the observed level bending and space charge layer width agree well with the concept of standard semiconductor theory. The additionally observed interface dipole and the ionization potential of the organic layers are not changed upon doping.

## Acknowledgements

We thank M. Knupfer, J. Fink, N. Karl and D. Wöhrle for stimulating and helpful discussions. Support by a joint DAAD-NSF program and a SMWK Graduiertenstipendium (J.B.) is acknowledged.

## References

[1] M. Pope, C.E. Swenberg, Electronic Processes in Organic Molecular Crystals, Oxford University Press, New York, 1999.
[2] S. Forrest, Chem. Rev. 97 (1997) 1793.
[3] C.W. Tang, S.A. VanSlyke, Appl. Phys. Lett. 51 (1987) 913.
[4] R.H. Friend, R.W. Gymer, A.B. Holmes, J.H. Burroughes, R.N. Marks, C. Taliani, D.D.C. Bradley, D.A. Dos-Santos, J.L. Brédas, M. Löglund, W.R. Salaneck, Nature 397 (1999) 121.
[5] H. Ishii, K. Sugiayama, E. Ito, K. Seki, Adv. Mater. 11 (1999) 605.
[6] Y. Park, V. Choong, E. Ettedgui, Y. Gao, B.R. Hsieh, T. Wehrmeister, K. Müllen, Appl. Phys. Lett. 69 (1996) 1080.
[7] S.T. Lee, X.Y. Hou, M.G. Mason, C.W. Tang, Appl. Phys. Lett. 72 (1998) 1593.
[8] I.G. Hill, A. Rajagopal, A. Kahn, J. Appl. Phys. 84 (1998) 3236.
[9] T. Mori, H. Fujikawa, S. Tokito, Y. Taga, Appl. Phys. Lett. 73 (1998) 2763.
[10] R. Schlaf, B.A. Parkinson, P.A. Lee, K.W. Nebesny, N.R. Armstrong, Appl. Phys. Lett. 73 (1998) 1026.
[11] R. Schlaf, B.A. Parkinson, P.A. Lee, K.W. Nebesny, N.R. Armstrong, J. Phys. Chem. B 103 (1999) 2984.
[12] A. Rajagopal, C.I. Wu, A. Kahn, J. Appl. Phys. 83 (1998) 2649.
[13] S.T. Lee, Y.M. Wang, X.Y. Hou, C.W. Tang, Appl. Phys. Lett. 74 (1999) 670.
[14] I.G. Hill, A. Kahn, J. Appl. Phys. 84 (1998) 5583.
[15] J.R. Waldrop, R.W. Grant, Phys. Rev. Lett. 43 (1979) 1686.
[16] K. Horn, Appl. Phys. A 51 (1990) 289.
[17] M. Maitrot, G. Guillaud, B. Boudjema, J.J. André, J. Simon, J. Appl. Phys. 60 (1986) 2396.
[18] J.J. André et al., Synth. Metal. 18 (1987) 683.
[19] D.R. Kearns et al., J. Chem. Phys. 32 (1960) 1020.
[20] T.J. Marks, Science 227 (1985) 881.
[21] E.J. Lous et al., Phys. Rev. B Condens. Matter 51 (1995) 17251.
[22] M. Pfeiffer, A. Beyer, T. Fritz, K. Leo, Appl. Phys. Lett. 73 (1998) 3202.
[23] A. Nollau, M. Pfeiffer, T. Fritz, K. Leo, J. Appl. Phys. 87 (2000) 4340.
[24] J. Blochwitz, M. Pfeiffer, T. Fritz, K. Leo, Appl. Phys. Lett. 73 (1998) 729.
[25] X. Zhou, M. Pfeiffer, J. Blochwitz, A. Werner, A. Nollau, T. Fritz, K. Leo, Appl. Phys. Lett. 78 (2001) 410.
[26] M. Pfeiffer, T. Fritz, J. Blochwitz, A. Nollau, B. Plönnigs, A. Beyer, K. Leo, Adv. Solid State Phys. 39 (1999) 77.
[27] G. Ertl, J. Küppers, Low Energy Electrons and Surface Chemistry, second ed., VCH Verlagsgesellschaft mbH, Weinheim, Deerfield Beach, 1985, Chapter 3.2.2.
[28] R. Schlaf, P.G. Schröder, M.W. Nelson, B.A. Parkinson, C.D. Merritt, L.A. Crisafulli, H. Murata, Z.H. Kafafi, Surf. Sci. 450 (2000) 142.
[29] I.H. Campbell, T.A.Z.S. Rubin, J.D. Kress, R.L. Martin, D.L. Smith, N.N. Barashkov, J.P. Ferraris, Phys. Rev. B 54 (1996) R14321.
[30] I.G. Hill, J. Schwartz, A. Kahn, Organic Electronics 1 (1) (2000) 5.
[31] K.F. Brennan, The Physics of Semiconductors, Cambridge University Press, Cambridge, New York, 1999.
[32] B. Boudjema, N. El-Khatib, M. Gamoudi, G. Guillaud, M. Maitrot, Rev. Phys. Appl. 23 (1988) 1127.
[33] H. Peisert, T. Schweiger, M. Knupfer, M.S. Golden, J. Fink, J. Appl. Phys. 88 (2000) 1535.
[34] Y. Park, V.-E. Choong, B.R. Hsieh, C.W. Tang, T. Wehrmeister, K. Müllen, Y. Gao, J. Vac. Sci. Technol. A 15 (1997) 2574.
[35] H. Ishii, H. Oji, E. Ito, N. Hayashi, D. Yoshimura, K. Seki, J. Lumin. 87–89 (2000) 61.
[36] I.G. Hill, A.J. Mäkinen, Z.H. Kafafi, Appl. Phys. Lett. 77 (2000) 1825.
[37] J.S. Kim et al., J. Appl. Phys. 84 (1998) 6859.
[38] F.R. Fan, L.R. Faulkner, J. Chem. Phys. 69 (7) (1978) 3334.
[39] S. Günster et al., Mol. Cryst. Liq. Cryst. Sci. Technol. A 218 (1992) 117.
[40] M. Pfeiffer, Controlled doping of organic vacuum deposited dye layers: basics and applications, Ph.D. Thesis, Technical University of Dresden, 1999.